From Single Droplet to Spray Wall Interaction – Multiple Droplet Chains

A. Müller*, E. Velios, K. Dullenkopf and H.-J. Bauer
Institut für Thermische Strömungsmaschinen
Universität Karlsruhe (TH)
Karlsruhe, Germany

Abstract

The further development of internal combustion engines is aimed towards higher efficiency and lower emissions. To achieve this goal, a detailed understanding of the mixture formation process is a crucial prerequisite. To enhance mixing and combustion quality, a general trend to higher fuel injection pressures, which leads to generation of droplets in a range below 20 µm, is evident. In the effort to study more realistic conditions and to achieve a more realistic database, the steps from single droplet over droplet chain experiments and now to multiple chain experiments have been made at the ITS. In this paper, the experimental setup and the results of a study under conditions as realistic as possible for DISI engines, with elevated pressure up to 3 bar, a heated wall element and droplets in the 80 µm scale are described. The wall element and the droplet chain generators are contained in a pressure vessel with adequate optical access. To simplify the complex spray and to allow extensive detailed measurements, up to three droplet chain generators are used, producing monodisperse equidistant droplets under elevated pressure. The droplets in this setup are slower and bigger compared to a DISI engine, but the resulting Reynolds number is in the range from 1500 to 2500 and therefore in the relevant range. This setup establishes well-defined boundary conditions and allows examination of the impingement process in detail.

Introduction

When performing experiments to investigate droplet-wall-interaction, there is always a trade-off. On one extreme, it is favorable to have experimental conditions as close as possible to reality. This means using a polydisperse spray, real fuel, elevated pressure, a hot moving piston head etc., but those conditions are difficult to access. Carrying out modeling is as difficult. On the other extreme, using single droplets is rather practicable and modeling can be performed very well [1, 3]. Closing the gap and transferring models found there to real conditions is hardly possible and questionable.

There are some steps in-between to close the gap. One measure that is still practicable is to use droplet chains [2, 4]. This adds more fuel impulse/mass flow, a wetted wall and temporal interaction to the scenery. To investigate spatial interaction, one approach is to use a single substrate that has several drill holes as orifices and therefore generates several parallel droplet chains [2]. With different drill patterns, varying impact distances can be studied. The difficult feature here is that drill tolerances turn out to make the trajectories as well as the impact time scattering.

In this paper, a new setup with three independently adjustable droplet chain generators is presented. All three droplet chains can be concentrated on one impingement location, or the spatial impact pattern can even be adjusted. Additionally, the timing of each droplet chain can be tuned individually and thus achieving a simultaneous impact from all chains.

Experimental Setup

The experimental setup consists of three main components (Figure 1): A triad of droplet chain generators producing equidistant chains of monodisperse primary droplets that serve as an abstraction for a DISI spray; a pressure vessel to perform measurements at the pressure level as in a cylinder during injection; and a heated stationary wall element as an analogy for the piston head where the spray is impinging in the real engine. Facts about the pressure vessel, droplet generation and the wall element are omitted here since they are already described in [4] in detail.

Compared to the previous setup that comprised only one droplet chain generator, several features were modified, as summed up in Table 1. Most obvious, the top cover of the pressure vessel has three supports for three identical droplet chain generators. Two micrometer screws per droplet chain generator have been added to adjust the azimuth and elevation of the droplet trajectory. Positioning accuracy is up to 10 µm at the impact location. The tip of the droplet chain generators, where the orifice is mounted, has been reworked to allow narrower spacing of the

*Corresponding author, armin.mueller@its.uni-karlsruhe.de

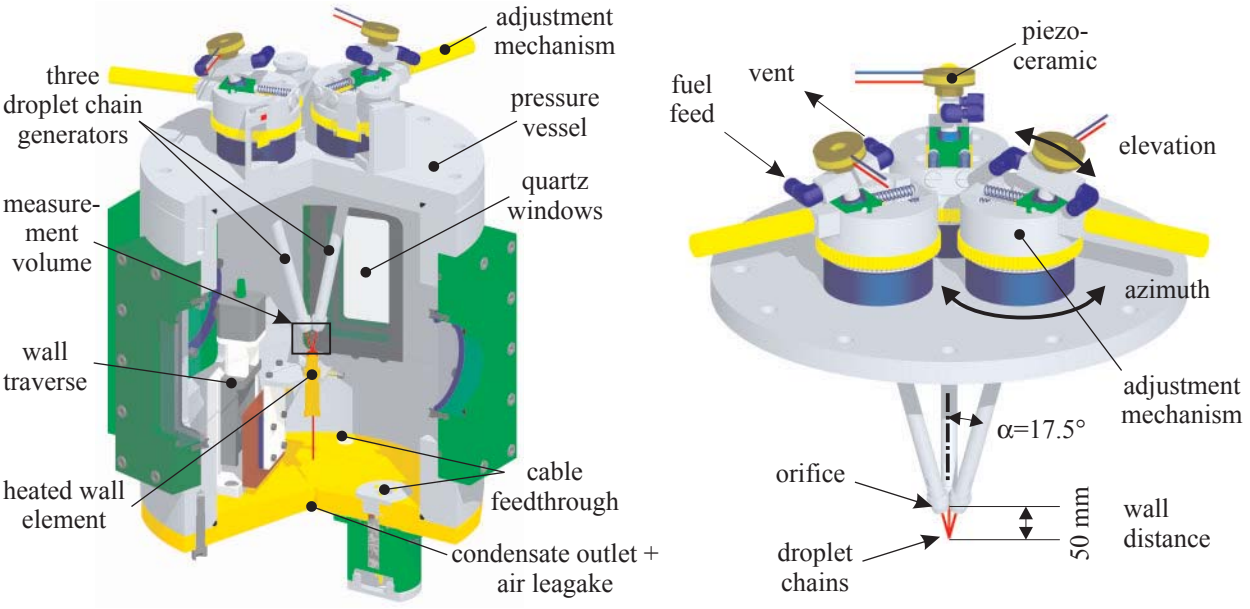

Figure 1. Experimental setup with pressure vessel and three droplet chain generators

trajectories. As a result, the three droplet chains can be concentrated on one point in a distance of 50 mm. The excitation of all three piezo-ceramic elements is controlled by a digital delay generator (Quantum Composers 9514+). All three droplet chains have the same excitation frequency f, but the phase can be adjusted to achieve a simultaneous impact at the wall.

Table 1. Comparison between old and new setup

Type of experiment	Number of droplet chains	Minimum wall distance	Angle of impact	Typical fuel mass flow
single	1	20 mm	Arbitrary	25 – 100 ml/h
triad	3	50 mm	$\alpha \geq 17.5°$	75 – 300 ml/h

Although this setup is more versatile than the old one and meets the demands, several drawbacks should be noted: The minimum distance between orifice and wall was increased, so with very small droplets or elevated pressure, the droplet chains are getting unstable before hitting the wall. The minimum impact angle is 17.5°, so one has to be careful when comparing results with other experiments that hit the wall vertically [5]. Last, but not least, the fuel mass flow is three times as high. This leads to more unwanted evaporation and Schlieren in the measurement volume as well as condensation at the windows, which is degrading image quality. Conducting the experiments was time consuming and exhausting, since the reliability of three droplet generators running concurrently is dramatically lower than of just one. Despite those difficult conditions, several series of measurement have been recorded successfully.

Isooctane was used as a surrogate for gasoline in all experiments, as it has well-defined physical properties and is less harmful than real fuel. The liquid properties of isooctane and gasoline are listed in Table 2 for comparison.

Table 2. Liquid properties of isooctane and gasoline for $T = 293$ K and atmospheric pressure.

Liquid	T_{sat} [K]	Density ρ [kg/m³]	Surface Tension σ [mN/m]	Dyn. Viscosity μ [µPa s]
Isooctane	372.4	688.8	18.2	466
Gasoline	273 – 483	700 – 740	23.0	399

Diagnostic Technique

As diagnostic technique, an extended particle tracking velocimetry (PTV) method was used [4, 6]. It simultaneously provides the 2D position, velocity and diameter of all droplets within the depth-of-field plane. Due to the

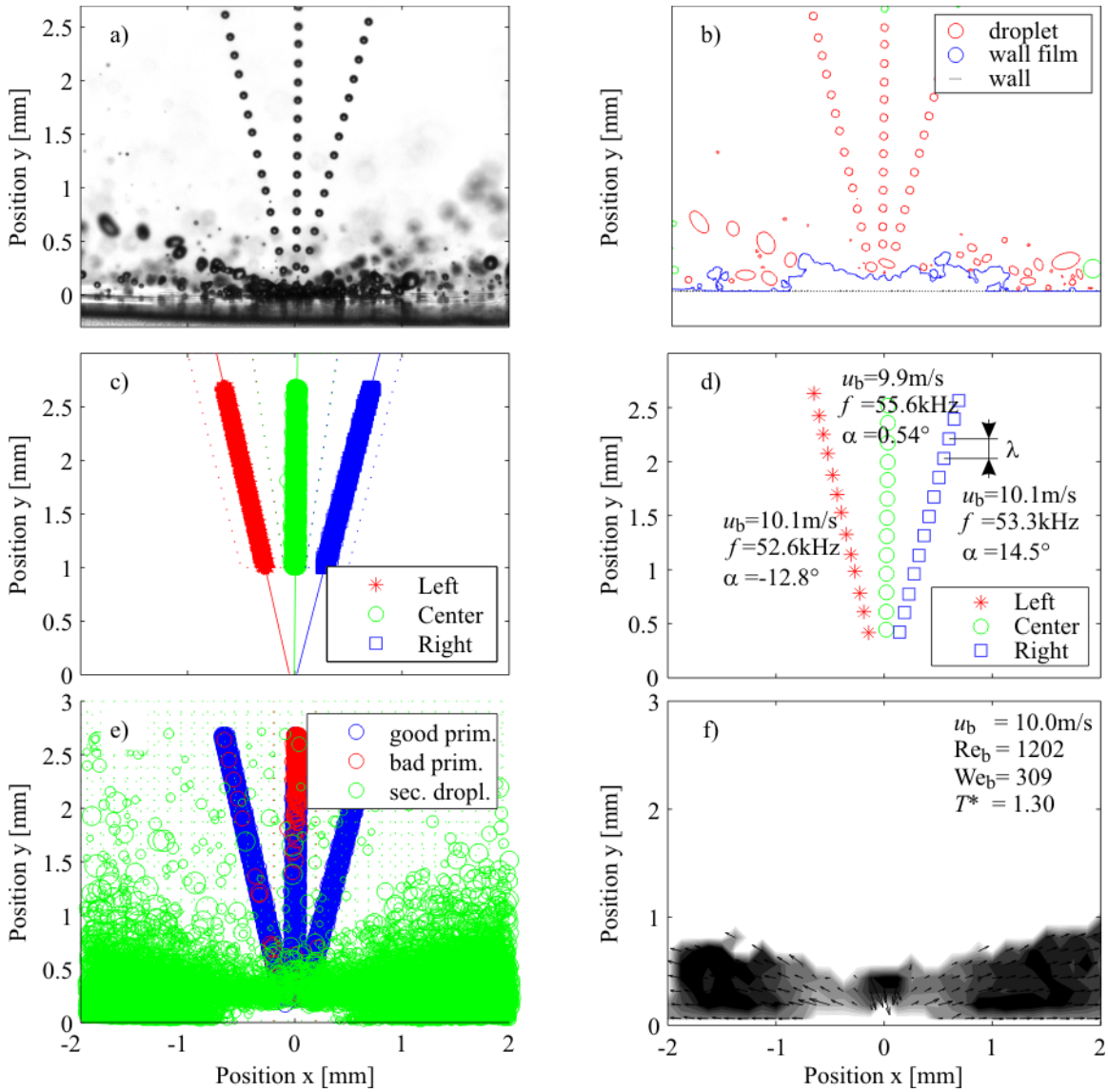

Figure 2. Analysis steps for the images

large magnification – the field of view measures only 4 mm × 3 mm – the depth-of-field is approximately in the range 50 to 120 µm. In contrast to simplistic algorithms used in other studies, the underlying algorithm in this paper is extended with a heuristic in such a way that it is capable to discriminate between background, wall, primary droplets, secondary droplets and the wall film.

The optical setup is basically a shadowgraphy setup. A dual cavity Nd:YAG pulse laser provided short time high power back light illumination. Laser energy was up to 2 × 120 mJ. The delay between the pulses was adjusted according to the operating conditions between $\Delta t = 3.5$ µs and 7 µs. The beam profile was broadened by an expansion lens and equalized in intensity by means of a diffuser disc. Due to interference effects, laser speckles are generated at the diffuser which would render the images useless. To overcome this phenomenon, a cuvette containing a laser dye was inserted into the optical path. It absorbed the coherent laser light and emitted incoherent light of a different wavelength and a very uniform intensity distribution. After crossing the measurement volume, the backlight was recorded by a standard double frame PIV camera.

The double frame images were analyzed by means of an automated processing in order to extract simultaneously and for the entire 2D-field information about droplet size, droplet position, droplet number, droplet velocity and film height (Figure 2). In contrast to other techniques, e.g. PDA, the droplets are not necessarily required to be spherical. Thus, for investigations near the wall, this technique yields significantly better results. The image analy-

sis is performed by a MATLAB code developed at ITS. This code is working in two phases. In the first phase, all double frame images are processed by an extended Particle Tracking Velocimetry (PTV) code. It is finding the contours of all objects by thresholding. The objects are coarsely classified in the categories wall film, droplets and background. Figure 2a and 2b give an example for that classification. The wall film is not further analyzed in this particular setup, because it is shaped too complex. For all droplets, the position, velocity and diameter are calculated. Position is calibrated using a scale paper. For the diameter, a calibration function is determined beforehand by means of a calibration target that contains circles in fine increments [6].

In the second phase, the droplets are further classified in the categories "good primary", "bad primary" and "secondary" droplets, which is not quite trivial. When working with just one droplet chain, the primary droplets move vertically downwards with the nominal speed. The secondary droplets move rather horizontally with moderate velocity. This is illustrated in Figure 3 (left). Depending on the operating point, for three droplet chains, the droplets can be very dense, move also vertically and are likely to collide with the primary droplets. Figure 3 (right) gives an impression. Therefore, the image is divided into three sectors. Droplets in each sector that have the anticipated velocity and diameter are collected (Fig. 2c). For each sector, a linear trajectory is fitted. Now every particle that is within a range of ±0.1 mm to that trajectory is counted as "good primary" droplet. Other droplets that are within ±0.25 mm to the trajectory are likely to be generated wrong or had a collision. Therefore they are labeled as "bad primary" droplets. The remaining droplets are "secondary" droplets. Figure 2e shows the classification for all 33,000 particles seen on all 300 images of this operating point. The primary droplet properties like diameter D_b, frequency f, velocity u_b and spacing $\lambda = u_b/f$ are known ahead. To double-check if everything was correct at recording time, those values are calculated from the images (Fig. 2d). It has to be considered that only 2D projections of the trajectories can be seen, so the velocities are corrected by perspective. Finally, histograms for the secondary droplets are generated, as is shown in Fig 2f.

Results and Discussion

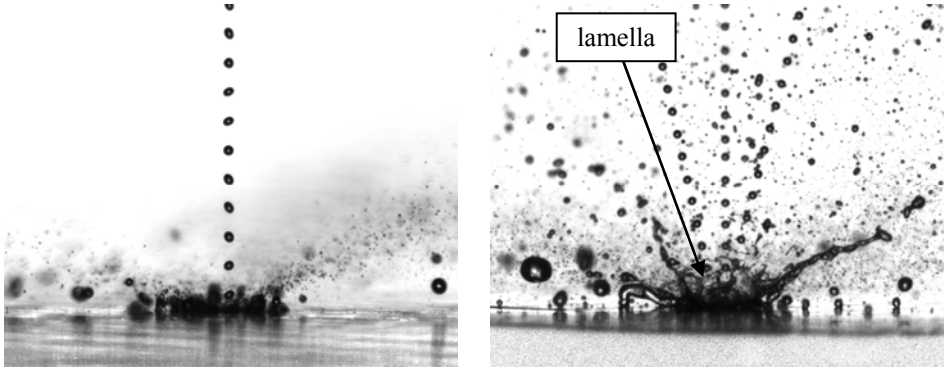

Figure 3. Sample images using a single droplet chain (left) and three droplet chains (right)

To give an impression of the difference between using a single and a triad of droplet chains, some typical images are illustrated in Fig. 3. It is to note that with just one droplet chain, not many details are visible within the liquid film (left). From the impact of three simultaneous droplet chains (right), it becomes apparent that – as it is the case with single droplets – a lamella is forming. This findings support the use of a semi-empirical model that has originally been developed for the description of a splashing single droplet [3] and has been found to give good agreement in a previous publication [4].

Several parameters were modified systematically. Exemplary, Fig. 4 is showing two columns with a variation of primary droplet velocity u_b (left) and wall temperature T^* (right). On the left side, velocity is varied from $u_b = 4.5$ m/s to 21.7 m/s. The primary droplet diameter is held constant with $D_b = 81$ µm. Therefore, the excitation frequency has to be adapted from $f = 33$ kHz to 100 kHz. Mass flow and impulse are changing accordingly. For low velocities, the impulse is too low. Nucleate boiling can be observed with big individual bubbles. At $u_b = 10$ m/s, the bubbles get more numerous, smaller and streaks occur. Above of the film, a lamella is visible. The regime changes to film boiling. This is in accordance with a single droplet chain [4]. For higher primary droplet velocities, more and smaller secondary droplets are generated. The spray cone angle is getting more flat.

On the right side, the dimensionless wall temperature $T^* = T_{wall}/T_{sat}$ is varied from $T^* = 1.13$ to 1.40. Again, the primary droplet diameter is held constant with $D_b = 81$ µm, frequency is $f = 53$ kHz, $u_b = 10$ m/s. For low wall tem-

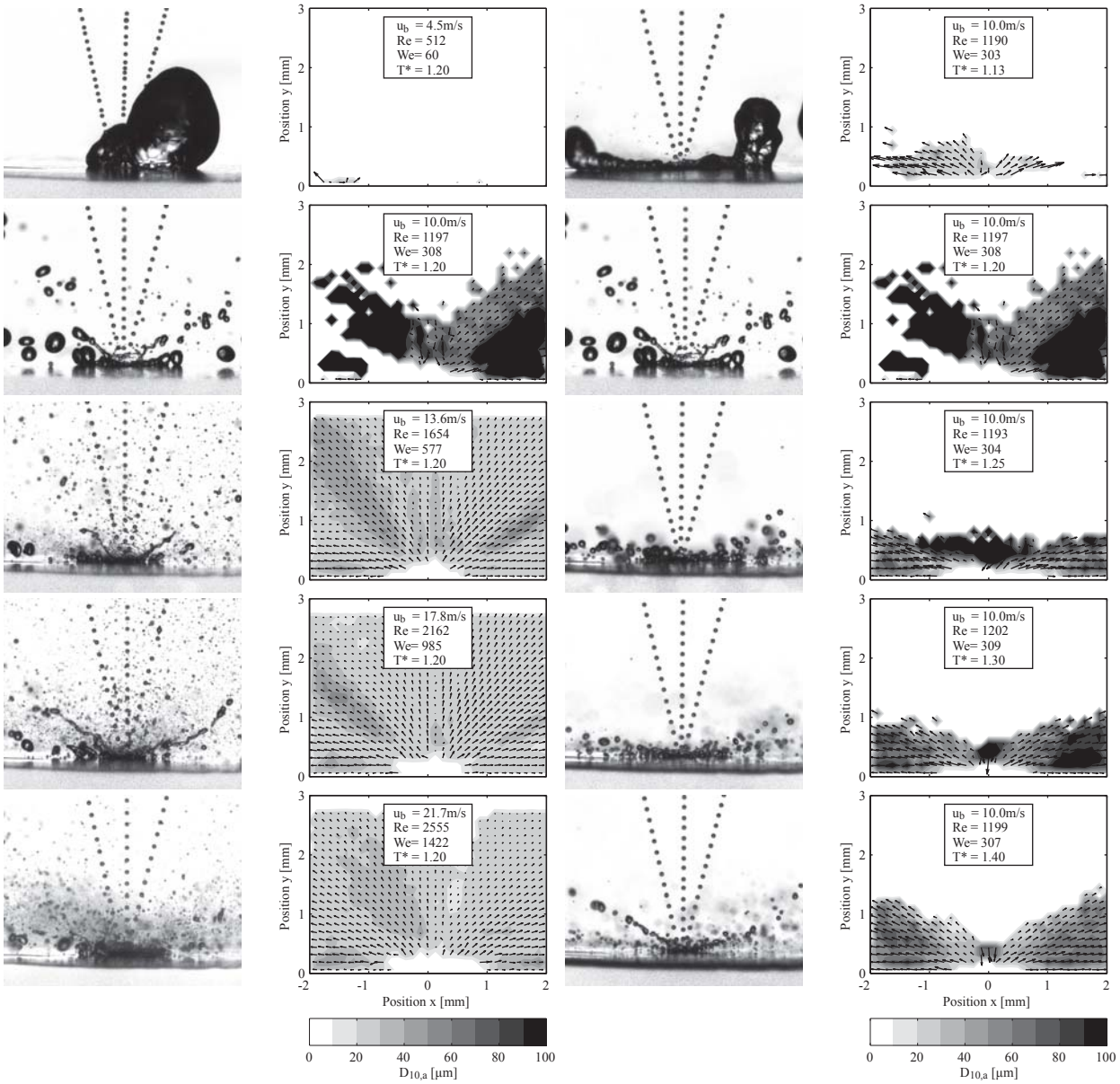

Figure 4. Variation of the primary droplet velocity u_b (left columns) and dimensionless wall temperature T^* (right columns) at atmospheric conditions

peratures, thermal energy is too low and nucleate boiling is occurring. Beginning at T^*=1.20, the nucleate bubbles get smaller and the regime changes to film boiling. At higher wall temperatures, the secondary droplets get smaller and slower. It seems that the small (thermal) secondary droplets are moving more parallel to the wall. At $T^* = 1.40$, a streak of larger secondary droplets is rising which is emerging infrequently.

Finally, a correlation was set-up for the diameter of the secondary droplets. Since the present case with high impact velocities represents an inertially dominated flow, the secondary droplet diameter is plotted as a function of the droplet impact Reynolds number $\mathrm{Re_b}$ (Figure 5) [3]. The symbols (○) correspond to data that was obtained with a single droplet chain at $T^* = 1.15$ and $p = 1$ bar and 3 bar ($T_{\mathrm{wall}} = 155$ °C and 207 °C) in previous work. The symbols (×) correspond to the data shown in Fig. 4 obtained with three droplet chains in the case where film boiling occurs at $T^* = 1.20$ and $p = 1$ bar as well as 3 bar ($T_{\mathrm{wall}} = 175$ °C and 228 °C). The arithmetic mean diameter of secondary droplets $D_{10,\mathrm{a}}$ can be determined by fitting the data as follows:

$$D_a = 16.8 \cdot D_b \cdot \mathrm{Re}_b^{-1/2} \qquad \text{with } \mathrm{Re}_b > 1600 \qquad (1)$$

It is to note that the fit for three droplet chains has a greater statistical spread than for the single droplet chain, but is still reasonable. Unfortunately, the Reynolds number could only be varied within a narrow band. This is due to the fact that only two sets (d = 30 µm and 40 µm) of orifices were at hand. The smaller orifices which would produce smaller droplets showed to be very susceptible to clogging. Effectively, only a turndown ratio of $p_{max}/p_{min} \approx 9$ for the pressure could be varied which results in a ratio of $u_{b,max}/u_{b,min} \approx 3$ for velocity. Within that range, only the operating points above $u_b \approx 11$ m/s show film boiling.

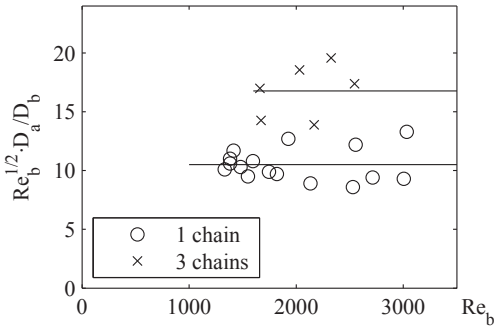

Figure 5. Average diameter D_a of the secondary droplets scaled by the diameter D_b of the primary droplets and Reynolds number, film boiling regime

Conclusion

Droplet-wall-interaction was studied in a setup closer to reality as many single droplet or single droplet chain configurations are able to achieve. By using three droplet chains simultaneously, the interaction of droplets in a relevant Reynolds number range could be investigated under elevated pressure on a heated wall element. Even for high wall temperatures, intensive interaction of droplets and the wetted wall could be analyzed by using high quality backlight imaging. This high quality images allowed discriminating the impact regime by the droplet formation morphology.

There is evidence that a lamella is forming after impingement. This is the first time a lamella was observed with droplet chain experiments, which has previously been observed only in single droplet experiments. In particular, the lamella is not visible when using a single droplet chain. These findings support the use of the Reynolds modeling approach, which was already found to give good agreement in a previous publication.

The same images were analyzed by means of an extended particle tracking velocimetry method to get quantitative experimental data of the secondary droplets, namely droplet position, number, velocity and diameter, for the whole field of observation. To predict secondary droplet diameters, an approach based on the Reynolds number has been strengthened. It has been shown that there is a difference between a single droplet chain and using a triad of droplet chains. Therefore, the new results allow a deeper insight to the physics and are helping to close the gap between single droplet experiments and real spray experiments in the understanding and the prediction of spray-wall-interaction.

Acknowledgements

The authors gratefully acknowledge the financial support for this project by the German Research Foundation (Deutsche Forschungsgemeinschaft, DFG) within the framework of the Collaborative Research Center SFB606 ”Unsteady Combustion: Transport phenomena, Chemical Reactions, Technical Systems”.

Nomenclature

d	m	orifice diameter
D	m	droplet diameter
f	1/s	frequency
p	bar	pressure
t	s	time
T	°C	temperature
u	m/s	droplet velocity
α	°	inclination angle
ρ	kg/m³	density
μ	Pa s	dynamic viscosity
σ	N/m	surface tension

Dimensionless numbers

$\mathrm{Re} = \rho D_b u_b / \mu$	Reynolds number
$\mathrm{We} = \rho D_b u_b^2 / \sigma$	Weber number

Subscripts

a	after impact
b	before impact
10	arithmetic mean
sat	saturation
wall	wall surface

References

1. Richter, B., Dullenkopf, K., and Wittig, S., Wall impact of single droplets under conditions of DISI-Engines. 9th Int. Conf. on Liquid Atomization and Spray Systems, Sorrento, Italy, 2003
2. Richter, B., Dullenkopf, K., and Bauer, H.-J., Investigation of secondary droplet characteristics produced by an isooctane drop chain impact onto a heated piston surface, Exp. Fluids 39:351-363 (2005)
3. Roisman, I.V., Horvat, K., and Tropea, C., Spray impact: Rim transverse instability initiating fingering and splash, and description of a secondary spray, Physics of Fluids 18:102104 (2006)
4. Müller, A., Schumann, F., Dullenkopf, K., and Bauer, H.-J., Analysis of Droplet Wall Interaction using Advanced Image Processing Techniques, Proc. 21st ILASS Europe, Muğla, Turkey, 2007
5. Moreira, A.L.N., Moita, A.S., Cossali, G.E., Marengo, M., and Santini, M., Secondary atomization of water and isooctane drops impinging on tilted heated surfaces. Exp. Fluids 43:297-313 (2007)
6. Kapulla, R., Tuchtenhagen, J., Müller, A., Dullenkopf, K., and Bauer, H.-J., Droplet Sizing Performance of Different Shadow Sizing Codes, Lasermethoden in der Strömungsmesstechnik, 15. Fachtagung, GALA e. V., Karlsruhe, Germany, 2008.